2016

Condensation Of Superheated R134a Inside A Vertical Tube

Jaime Sieres
Área de Máquinas y Motores Térmicos, Escuela de Ingeniería Industrial, University of Vigo, Spain, jsieres@uvigo.es

José Antonio Martínez-Suárez
Área de Máquinas y Motores Térmicos, Escuela de Ingeniería Industrial, University of Vigo, Spain, jambuscas@hotmail.com

Elena Martín
Área de Mecánica de Fluidos, Escuela de Ingeniería Industrial, University of Vigo, Spain, emortega@uvigo.es

Condensation of Superheated R134a Inside a Vertical Tube

Jaime SIERES[1]*, José Antonio MARTÍNEZ-SUÁREZ[1], Elena MARTÍN[2]

[1]Área de Máquinas y Motores Térmicos, Escuela de Ingeniería Industrial,
Campus-Universitario Lagoas-Marcosende, University of Vigo, 36310 Vigo, Spain
Phone: +34 986811997, Fax: +34 986811995, E-mail: jsieres@uvigo.es

[2]Área de Mecánica de Fluidos, Escuela de Ingeniería Industrial,
Campus-Universitario Lagoas-Marcosende, University of Vigo, 36310 Vigo, Spain
E-mail: emortega@uvigo.es

* Corresponding Author

ABSTRACT

An experimental study is performed to investigate condensation of superheated R134a inside a vertical tube. Experimental tests have been performed at the normal operating conditions found in a small power vapour compression refrigeration system. The experimental setup is described and the experimental procedure and data reduction method are explained. Experimental results of the condensation heat transfer coefficient are reported and discussed for different pressures, vapor mass flow rates and vapor degrees of superheating. The experimental heat transfer coefficients are also compared with those obtained using different correlations; it is found that the values are well predicted with the Chen correlation.

1. INTRODUCTION

The issue of film condensation heat transfer on vertical surfaces including vertical tubes has been of primary interest to researchers in the field of heat transfer because of its occurrence in a variety of engineering applications. It is in fact included in any undergraduate heat transfer book (Incropera and DeWitt, 2002 or Çengel, 2003) and state-of-the-art reviews are usually covered in specialized handbooks (Marto, 1998; Kedzierski *et al.*, 2003; or McNaught and Butterworth, 2002).

The pioneer work related with laminar film condensation was reported by Nusselt (1916) who made a theoretical analysis in terms of simple force and heat balances within the condensate film. Ever since the original work by Nusselt, there have been a lot of publications and improvements on the problem such as those related with the effect of thermophysical properties (Bromley, 1952), the effects of waves and turbulence or the effect of interfacial shear (Rohsenow *et al.*, 1956; Labuntsov, 1957; Sparrow and Gregg, 1963; Kutateladze, 1963; Chen *et al.*, 1987).

In vapor-compression refrigeration machines the refrigerant enters the condenser as a superheated vapor. The degree of superheating depends mainly on the compression process (isentropic efficiency) and on the pressure ratio, but normally ranges from 10ºC to 40ºC. Minkowycz and Sparrow (1966) performed an analytical investigation of laminar film condensation including the effect of superheating. They showed that for steam condensation the effect of superheating brings about only a slight increase in the heat transfer coefficient. Recently, Longo (2011) experimentally studied the effect of vapor superheating on hydrocarbon refrigerant condensation inside a brazed plate heat exchanger. He showed that superheated vapor heat transfer coefficients were from 5% to 10% higher than those of saturated vapor under the same refrigerant mass flux values.

The present paper investigates condensation of superheated R134a inside a vertical tube. Experimental tests have been performed at the normal operating conditions found in a small power vapour compression refrigeration system.

Experimental results of the condensation heat transfer coefficient are reported and discussed for different pressures, vapor mass flow rates and vapor degrees of superheating.

2. EXPERIMENTAL SET-UP

2.1 Description

The schematic diagram of the experimental setup is shown in Figure 1. It is basically a small power refrigeration system and a small water loop circuit.

The evaporator consists of a vertical copper tube of diameter 9.52/7.92 mm and 0.99 m length. The evaporator is covered with a flexible power heating cable that supplies a uniform heating power along the evaporator length. The total heating power supplied to the evaporator is adjusted by means of an AC power supply. The refrigerant flows vertically from the bottom to the top of the evaporator. The refrigerant enters the evaporator as a two-phase flow and leaves it as a superheated vapor flow. The degree of superheat at the evaporator outlet is controlled manually by a commercial thermostatic expansion valve.

The condenser consists of two concentric copper tubes of 1.036 m length which are oriented vertically. The inner and outer tubes are of diameters 15.87/14.13 mm and 9.52/7.92 mm, respectively. The refrigerant condensation takes place as it flows downwards inside the inner tube. Water is used as the cooling medium which flows through the annular space formed by the two concentric tubes, in countercurrent with the refrigerant flow.
The cooling water flows in a closed loop consisting of a circulating pump and a forced air-cooled heat exchanger, constructed with copper tube of 3/8" in staggered arrangement and continuous aluminum fins. The cooling water temperature can be adjusted by controlling the airflow supplied by the fan of the air-cooled heat exchanger by means of a variable frequency drive. The cooling water flow rate can be controlled manually by way of different hand-valves (not shown in Figure 1).

The compressor is a commercial hermetic compressor with a displacement of 3.13 cm^3 per revolution. The refrigerant volumetric flow rate can be controlled by varying the compressor supply frequency by means of a variable frequency drive.

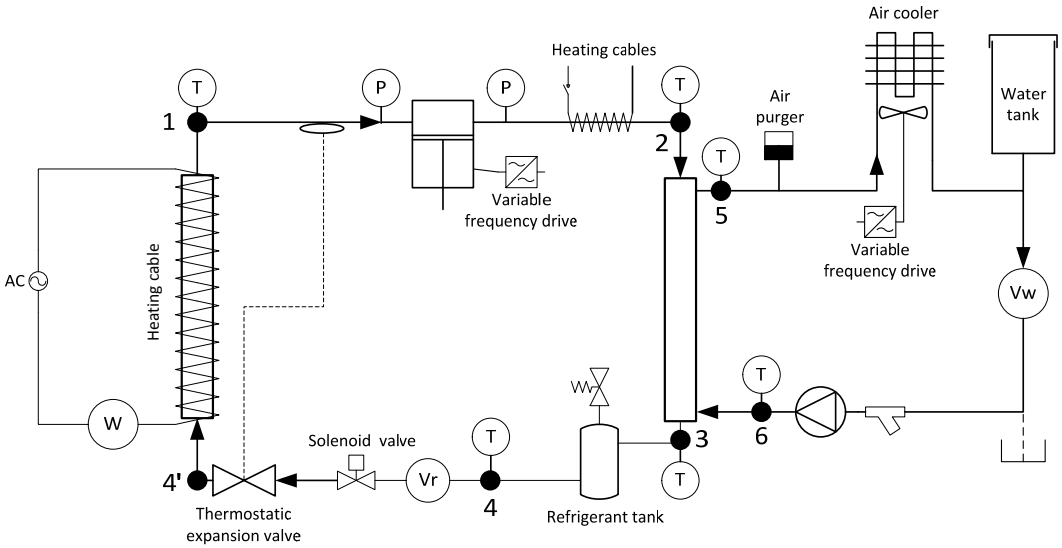

Figure 1: Schematic diagram of the experimental facility

Three small heating cables are coiled over the discharge pipe (between compressor and condenser) in order to control the degree of superheat at the condenser inlet. The connection of each heating cable to the mains power supply is controlled by a means of a solid state relay with an input control voltage between 3-15 VDC.

Other components of the refrigerant circuit of the experimental set-up are: high and low pressure gauges, a dual pressure control to protect the compressor against excessively low suction pressure or excessively high discharge pressure, a solenoid valve, a liquid line filter drier, a sight glass, a refrigerant liquid tank, a safety relief valve and proper instrumentation. The water loop circuit is also equipped with an air purge valve, a water tank, hand valves and proper instrumentation.

2.2 Data acquisition system

The experimental facility has been equipped with a supervisory control and data acquisition (SCADA) system based on a PC and an acquisition data card.

Four Pt100 sensors (type A) are installed on different points of the refrigerant circuit. These sensors measure the temperature at the evaporator outlet (T_1), compressor outlet (T_2), condenser outlet (T_3) and at the exit of the refrigerant tank (T_4). There are also two Pt100 sensors in the water loop circuit in order to measure the water flow temperature that enters (T_6) and exits (T_5) the condenser. Head mounted temperature transmitters are used for the six Pt100 sensors. The accuracy of the temperature transducers is ± 0.1 °C ± 0.05 % of reading.

The evaporator pressure (p_1) is measured with a pressure transducer in the range 0-6 bar and accuracy ±0.5% of the full scale. The condenser pressure (p_2) is measured with a pressure transducer in the range 0-25 bar and accuracy ±0.5% of the full scale. The atmospheric pressure is measured with a barometric pressure sensor with an accuracy of ±0.3 hPa.

The cooling water volumetric flow rate in the water loop is measured by means of an ultrasonic type flow meter (V_{cw}) in the range 0.08-20 L/min. The accuracy of the volumetric flow rate measurement within the operating range is ±1.5% of the full scale.

The refrigerant mass flow rate in the refrigerant loop is measured by means of turbine type flow meter (V_r) in the range 2-20 L/h. The accuracy of the volumetric flow rate measurement within the operating range is ±0.25% of the measured value.

The total heating power supplied to the evaporator is adjusted by means of an AC power supply. The power is measured by means of a single phase active power transducer (W). The measuring range of this transducer is 0-1000 W, with an accuracy of ± (0.45% reading + 0.05% full scale).

All sensors are scanned within a time interval of 2 s with an acquisition data card of 16 bits for analogical to digital conversion. The SCADA system allows a manual or automatic control of the output frequency from the variable speed drives used to run the compressor and the fan (of the air-cooler). In this work, the compressor frequency was set manually while the frequency for the fan of the air-cooler was automatically adjusted by means of a PID controller in order to regulate the condenser pressure. The SCADA system also allows controlling the degree of superheating at the condenser inlet by adjusting the number and interval time of the 3 heating cables installed on the discharge pipe.

2.2 Experimental procedure

The water flow rate, the static degree of superheat at the outlet of the evaporator and the heat power supplied to the evaporator were set manually for each experiment. The cooling water flow rate was controlled manually by way of the different hand-valves; the static superheat was adjusted manually by rotation of the side stem of the valve; whereas the power supplied to the evaporator was controlled manually by modifying the power output of the AC power supply.

Initially, different sets of experiments were performed for fixed values of the condensation pressure, while increasing the power in the heating cable of the evaporator in intervals of 25 W, from 50 W to 350 W, approximately. Moreover, the compressor frequency, the water flow rate and the rotation of the side stem of the thermostatic valve were also kept constant during these experiments. However, it was observed that when the heat power supplied to the evaporator was increased, the degree of superheat at the compressor outlet (or condenser inlet) increased rapidly and then remained nearly constant for further increasing values of the heat power. Then, in order to control the degree of superheat at the compressor outlet, it was necessary to act on the compressor supply frequency by means of the compressor variable frequency drive and on the heating cables installed on the discharge

pipe. A coarse adjustment of the superheat at the compressor outlet was made manually by changing the compressor supply frequency from the SCADA system. This coarse adjustment was based on the fact that when the compressor supply frequency increases the suction pressure decreases, leading to higher compressor discharge temperatures; higher discharge temperatures is equivalent to higher values of the degree of superheat, since the discharge pressure is constant (by virtue of the PID controller acting on the fan supply frequency). Then, the compressor supply frequency was adjusted in order to guarantee a degree of superheat some degrees lower than the set point value. The final value of the degree of superheat was obtained by controlling the heating cables power on the discharge pipe.

At the beginning of each experiment a frequency value for the compressor and a condenser pressure were established by means of the SCADA system. The PID controller of the SCADA system acted continually on the fan frequency value in order to guarantee the preset condenser pressure. For those experiments were a specific value of the superheat degree at the compressor outlet was desired, the compressor speed was changed manually and then a second PID controller was activated which acted on the heating cables of the discharge pipe in order to guarantee the preset superheat degree value.

It should be noted that experiments could only be done for some specific range of values of the heat power and condenser pressure. For decreasing values of the heat power supplied to the evaporator, the pressure of the vapour in the compressor suction line also decreases. Then, the minimum heat power was limited by the action of the low-pressure cut-out switch. On the other hand, the maximum heat power was limited by the preset condenser pressure and the ambient temperature. These limits were somehow affected by the compressor supply frequency.

During each experiment, steady state conditions were confirmed by visualizing the measured variables in the SCADA system. In general, steady state operation was reached within a period of 2-3 hours. Thereafter, data recording during the next 40-60 minutes was performed for all the measured variables.

Figure 2 shows the experimental values for a characteristic experimental test of the power supplied to the heating cable in the evaporator and the water flow rate through the condenser. These two values were fixed manually for each experiment. However, small variations of the heat power supplied to the evaporator were observed during each experiment which was attributed to the voltage stability of the electrical grid. Also, the volumetric flow rate varied slightly during an experiment because of the temperature variation of the water flow rate. In general, these variations were rather low for a 40-60 minutes period of the data recording process (lower period than in the figure).

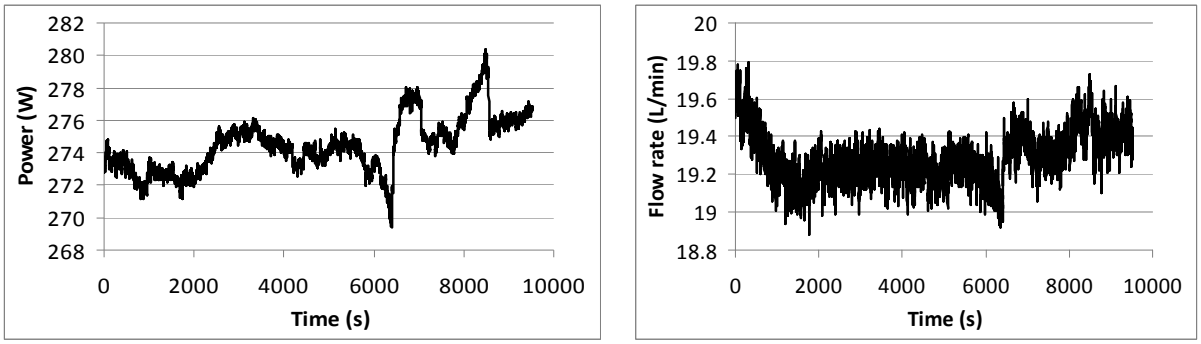

Figure 2: Experimental values of the power supplied to the heating cable in the evaporator and the water flow rate through the condenser

Figure 3 shows the experimental values for a characteristic experimental test of the refrigerant (T_2 and T_3) and water temperatures (T_5 and T_6) at the inlet and outlet of the condenser and of the condenser pressure. In this case, steady-state operating conditions were obtained after 1.5-2 hours of the beginning of the test.

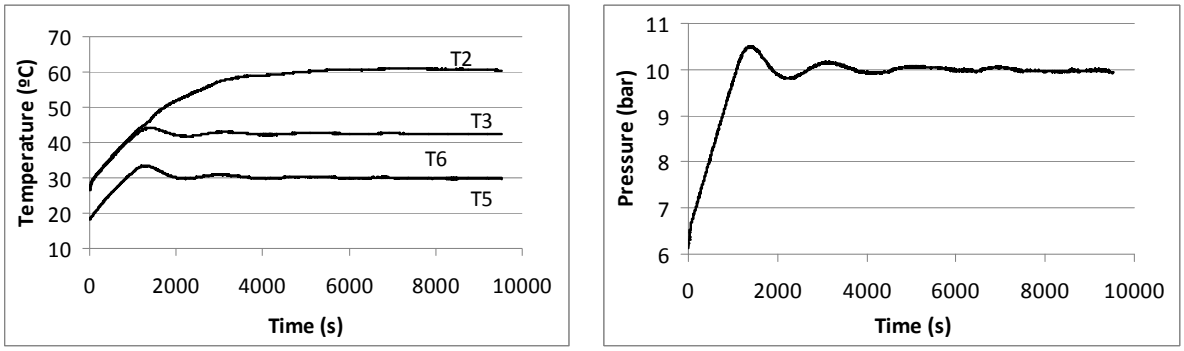

Figure 3: Experimental measured values of the refrigerant and water temperatures at the inlet and outlet of the condenser and the condenser pressure for a characteristic test run

3. DETERMINATION OF HEAT TRANSFER COEFFICIENTS

From the measured data in the experimental setup, the thermodynamic conditions of the refrigerant and the water at the various states of the system are determined at steady state conditions. The state conditions at the inlet of the evaporator are determined from the state conditions of the refrigerant at the outlet of the refrigerant tank and assuming an isenthalpic process in the thermostatic valve. All refrigerant and water properties were obtained using the REFPROP Database (Lemmon *et al.*, 2010).

The refrigerant mass flow rate can be determined from the refrigerant volume flow-meter and the refrigerant (liquid) density at the outlet of the refrigerant tank.

$$\dot{M} = \dot{V}_r \cdot \rho_4 \tag{1}$$

The heat transfer rate in the condenser is determined using equation (2).

$$\dot{Q}_{cond} = \dot{M} \cdot (h_2 - h_3) \tag{2}$$

Once the heat transfer rate in the condenser is determined, the overall thermal resistance (R_{ov}) is obtained from equation (3) where the logarithmic mean temperature difference is given by equation (4).

$$\dot{Q}_{cond} = \Delta T_{lm} / R_{ov} \tag{3}$$

$$\Delta T_{lm} = \frac{T_5 - T_6}{\ln\left(\frac{T_{cond} - T_6}{T_{cond} - T_5}\right)} \tag{4}$$

In equation (4), T_{cond} is the refrigerant saturation pressure at the condenser pressure. Due to the small dimensions of the condenser, pressure drops were neglected.

The overall thermal resistance is the sum of three thermal resistances: the thermal resistance of the refrigerant condensation process, the thermal resistance of the tube wall against heat conduction and the thermal resistance of the cooling water side convection process inside a tube annulus.

$$R_{ov} = R_c + R_w + R_{cw} \tag{5}$$

$$R_c = \frac{1}{h_c \cdot A_i} = \frac{1}{h_c \cdot \pi \cdot D_i \cdot L_{cond}} \tag{6}$$

$$R_w = \frac{\ln(D_e/D_i)}{2 \cdot \pi \cdot L_{cond} \cdot k_w} \tag{7}$$

$$R_{cw} = \frac{1}{h_{cw} \cdot A_e} = \frac{1}{h_{cw} \cdot \pi \cdot D_e \cdot L_{cond}} \tag{8}$$

During all the experiments, fully developed turbulent flow was obtained for the water annular flow in the condenser. The water side heat transfer coefficient is determined by the Petukhov and Roizen (1964) correlation. Once the water-side heat transfer coefficient is determined, then the condensation heat transfer coefficient on the inside surface of the tube can be obtained from equation (9).

$$h_c = \frac{1}{R_{ov} \cdot \pi \cdot D_i \cdot L_{cond} - \frac{D_i \cdot \ln(D_e/D_i)}{2 \cdot k_w} - \frac{D_i}{h_{cw} \cdot D_e}} \tag{9}$$

4. RESULTS AND DISUSSION

Experiments were carried out with heat powers from 50 W to 350 W, condenser pressures from 8 to 13 bar and superheating degrees at the condenser inlet between 10 and 30 ºC. The cooling water flow rate for all experiments was kept nearly at a constant value of 20 L/min.

Figures 4 and 5 show the condensation heat transfer coefficient as a function of the condensate Reynolds number for different condenser pressures and constant values of the superheating degree of 10 ºC and 20 ºC, respectively. The condensate Reynolds number used in these figures is calculated at the bottom of the tube (exit section), according to equation (10).

$$Re_c = \left(4 \cdot \dot{M}\right)/(\pi \cdot D_i \cdot \mu_l) \tag{10}$$

For each pressure, different tests were made varying the compressor supply frequency within 35-60 Hz. A detailed analysis of the experimental uncertainties was carried out and the typical uncertainty bands (with a coverage factor $k = 1$) are included in the figure. The uncertainties have been determined from the analysis of the experimental measurements and the accuracy specifications of the different sensors, as indicated in ISO (1995). For the water side heat transfer coefficient an uncertainty of 15% was considered, based on the comparison of the Petukhov and Roizen correlation with the experimental data of several authors (Gnielinski, 2002).

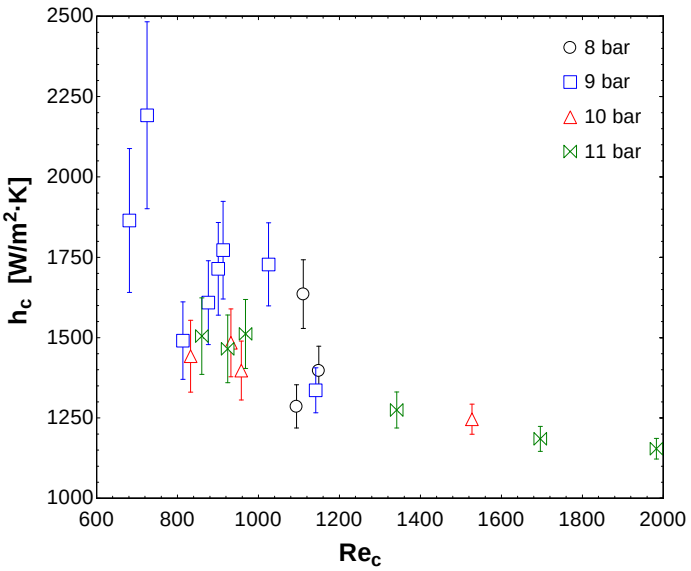

Figure 4: Experimental condensation heat transfer coefficients as a function of the condensate Reynolds number for a set of experiments carried out for a constant superheating degree of 10ºC and different condensation pressures

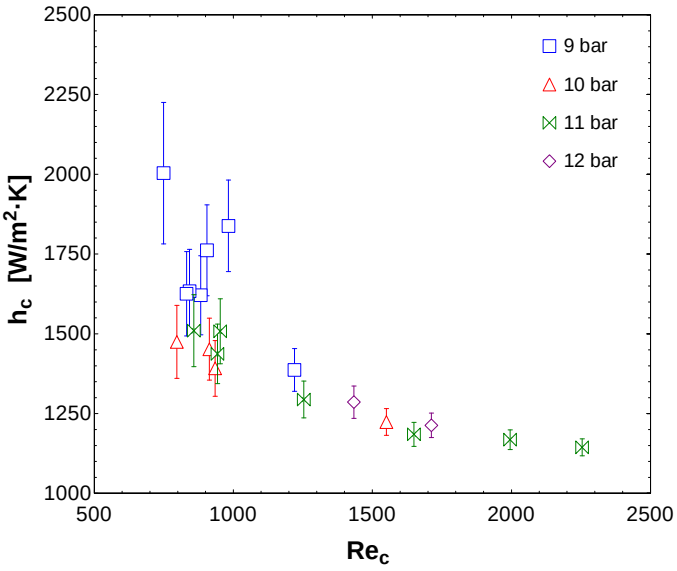

Figure 5: Experimental condensation heat transfer coefficients as a function of the condensate Reynolds number for a set of experiments carried out for a constant superheating degree of 20ºC and different condensation pressures

It should be noted that the condenser design and operating conditions were selected in order to ensure that the tube wall and water-side thermal resistances are much lower than the refrigerant side thermal resistance. As a result, the 15% uncertainty value assigned to the water side heat transfer coefficient has a low impact on the uncertainty of the refrigerant side heat transfer coefficient calculation. Anyway, its effect becomes more important for low refrigerant Reynolds numbers due to the higher (lower) refrigerant heat transfer coefficients (thermal resistance) obtained for the low Reynolds experiments, as confirmed in figures 4 and 5.

Comparing the four pressure series of experimental results in figures 4 and 5, it can be stated that the condenser pressure has no effect on the experimental values of the condensation heat transfer coefficient. Also, results in Figure 4 suggest that for the Reynolds numbers above 1200 (approx.), the Reynolds number has a mild effect on the heat transfer coefficient, decreasing slightly with increasing values of the Reynolds number. However, for Reynolds numbers below 1200, the effect of the Reynolds number is more evident.

Figure 6 shows experimental results of the heat transfer coefficient for different superheating degree values at the condenser inlet. From the results shown in this figure, it can be stated that the superheating degree has not a clear effect on the condensation heat transfer coefficient.

The experimental values of the condensation heat transfer coefficient were compared with those obtained using different correlations, such as: the Nusselt's theory (1916) for laminar flow, the correlations in McNaught and Butterworth (2002) for wavy laminar or turbulent flow, and the Chen (1987) correlation. The first two correlations are for gravity-dominated flow (neglecting the vapor drag on the liquid film) whereas the Chen correlation takes into account the combined effects of the vapor interfacial shear and gravity.

The condensation heat transfer coefficient for wavy laminar or turbulent flow is calculated by equations (11) or (12) as a function of the Reynolds number.

$$Nu = \frac{Re_c}{1.08 \cdot Re_c^{1.22} - 5.2}, Re_c \leq Re_{trans} \tag{11}$$

$$Nu = \frac{Re_c}{414.59 \cdot Re_c^{0.6} \cdot Pr_l^{-0.65} - 5.182 - 33514 \cdot Pr_l^{-1.28}}, Re_c > Re_{trans} \tag{12}$$

where the transitional Reynolds number given by equation (13).

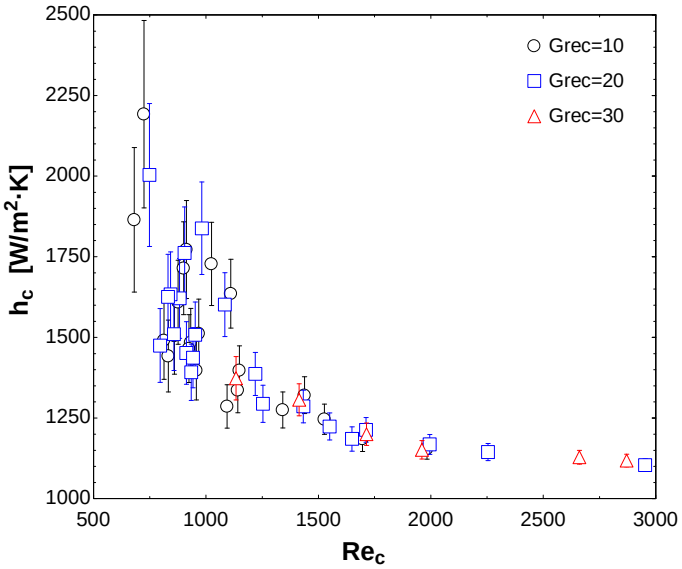

Figure 6: Experimental condensation heat transfer coefficients as a function of the condensate Reynolds number for a set of experiments carried out with superheating degrees of 10ºC, 20ºC and 30ºC

$$Re_{trans} = 4658 \cdot Pr_l^{-1.05} \tag{13}$$

In these correlations the Nusselt number is given by:

$$Nu = \frac{h_c}{k_l} \cdot \left(\frac{\mu_l^2}{g \cdot \rho_l \cdot (\rho_l - \rho_v)} \right)^{1/3} \tag{14}$$

The Chen correlation is given by equation (15).

$$Nu = \left(Re_c^{-0.44} + \frac{Re_c^{0.8} \cdot Pr_l^{1.3}}{1.718 \cdot 10^5} + \frac{C \cdot Pr_l^{1.3} \cdot Re_c^{1.8}}{2075.3} \right)^{0.5} \tag{15}$$

where:

$$C = \frac{0.252 \cdot \mu_l^{1.177} \cdot \mu_v^{0.156}}{D_i^2 \cdot g^{0.667} \cdot \rho_l^{0.553} \cdot \rho_v^{0.78}} \tag{16}$$

Figure 7 shows the experimental values of the condensation heat transfer coefficient and those obtained from the previous correlations, as a function of the Reynolds number. Results show that the experimental values of h_c are much higher than those obtained with the Nusselt theory, but similar to those obtained by the wavy laminar-turbulent and Chen correlations. Moreover, for the low Re_c range of experiments the Chen correlation seems to predict better the experimental results, though the experimental uncertainties in this region is much higher than for the higher Re_c experiments. Finally, the experimental results and also the last two correlations predict a decreasing value of h_c with Re_c up to values of Re_c around 2000, for higher Re_c values but then h_c remains nearly constant.

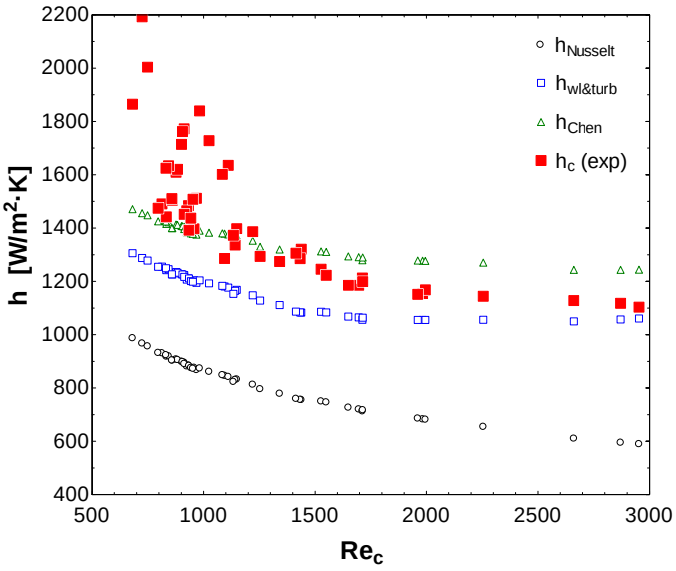

Figure 7: Experimental values of the condensation heat transfer coefficient as a function of the condensate Reynolds number and predicted values from different correlations

6. CONCLUSIONS

This paper deals with the condensation of superheated R134a inside a vertical tube. Experimental tests have been performed at the normal operating conditions found in a small power vapor compression refrigeration system. Experimental results of the condensation heat transfer coefficient are reported for different pressures, vapor mass flow rates and vapor degrees of superheating. Results were obtained for condensate Reynolds number between 500 and 3000 which corresponds to the Reynolds region were transition from wavy laminar to turbulent flow occurs. It was shown that experimental values of the condensation heat transfer coefficient are unaffected by the condenser pressure. The effect of the superheating degree is not clear taking into account the range of conditions tested and the uncertainties of the experimental heat transfer coefficients. Experimental results of the condensation heat transfer coefficient are in accordance with the Chen correlation.

NOMENCLATURE

The nomenclature should be located at the end of the text using the following format:

A	surface area	(m^2)
D	diameter	(m)
g	gravitational acceleration	(m/s^2)
h	specific enthalpy	(J/kg)
h	heat transfer coefficient	(W/m^2-K)
k	thermal conductivity	(W/m K)
L	length	(m)
$\dot{M}$	mass flow rate	(kg/s)
Nu	Nusselt number	(-)
p	pressure	(bar)
Pr	Prandtl number	(-)
R	thermal resistance	(K/W)
Re	Reynolds number	(-)
T	temperature	(ºC, K)
$\dot{Q}$	heat power	(W)
$\dot{V}$	volumetric flow rate	(m^3/s)
$\dot{W}$	power	(W)

Greek symbols

μ	dynamic viscosity	(kg/m-s)
ρ	density	(kg/m^3)

Subscript

c	condensation
cond	condenser
cw	cooling water
e	external
elec	electrical
evap	evaporator
i	internal
l	liquid
lm	logarithmic mean
ov	overall
r	refrigerant
trans	transitional
v	vapor
w	wall

REFERENCES

Bromley, L.A. (1952). Effect of heat capacity of condensate in condensing. *Ind. Engng. Chem.*, 44, 2966-2969.

Çengel, Y.A. (2003). *Heat transfer: a practical approach*. New York: McGraw-Hill

Chen, S. L., Gerner, F. M. & Tien, C. L. (1987). General film condensation correlations. *Exp. Heat Transfer*, 1, 93-107.

Gnielinski, V. (2002) Forced convection in ducts. In G.F. Hewitt (Ed.), *Heat Exchanger Design Handbook* (2.5.1-10).New York: Begell House.

Incropera, F. & DeWitt, D.P. (2002). *Introduction to heat transfer*. Hoboken, NJ: John Wiley & Sons

ISO (1995). *Guide to the Expression of Uncertainty in Measurement*. International Organization for Standardization

Kedzierski, M.A., Chato, J.C. & Rabas T.J. (2003). Natural convection. In A. Bejan & A.D. Kraus (Eds.), *Heat Transfer Handbook* (719-763). New York: Wiley.

Kutateladze, S.S. (1963). *Fundamentals of Heat Transfer*. New York: Academic Press Inc.

Labuntsov, D.A. (1957). Heat transfer in film condensation of pure steam on vertical surfaces and horizontal tubes. *Teploenergetika*, 4(7), 72-80.

Lemmon, E.W., Huber, M.L. & McLinden, M.O. (2010). *NIST Standard Reference Database 23: Reference Fluid Thermodynamic and Transport Properties-REFPROP v 9.0*. Gaithersburg, MD: National Institute of Standards and Technology (NIST), Standard Reference Data Program.

Longo, G.A. (2011). The effect of vapour super-heating on hydrocarbon refrigerant condensation inside a brazed plate heat exchanger. *Exp. Therm. Fluid Sci.*, 35(6), 978-985.

Marto, P.J. (1998). Condensation. In W.M. Rohsenow, J.P. Hartnett & Y.I. Cho (Eds.), *Handbook of Heat Transfer* (14.4-10). New York: Mc Graw-Hill.

McNaught, J.M. & Butterworth, D. (2002). Film condensation of pure vapour. In G.F. Hewitt (Ed.), *Heat Exchanger Design Handbook* (2.6.2.1-10). New York: Begell House.

Minkowycz W.J. & Sparrow, E.M. (1966). Condensation heat transfer in presence of noncondensables, interfacial resistance, superheating, variable properties, and diffusion. *Int. J. Heat Mass Transfer*, 9, 1125-1144.

Nusselt, W. (1916). Die oberflachenkondensation des wasserdampfes. *Z. Ver. Dtsch. Ing.*, 60, 541-575.

Petukhov, B.S. & Roizen, L.I. (1964). Generalized relationships for heat transfer in a turbulent flow of a gas in tubes of annular section. *High Temperature*, 2, 65-68.

Rohsenow, W.M. (1956). Heat transfer and temperature distribution in laminar film condensation. *Trans. Am. Soc. Mech. Engrs.*, 78, 1645-1648.

Rohsenow, W.M., Webber, J.H. & Ling, A.T. (1956). Effect of vapor velocity on laminar and turbulent film condensation. *Trans. ASME*, 78, 1637-1643.

Sparrow, E.M. & Gregg, J.L. (1959). A boundary-layer treatment of laminar film condensation. *J. Heat Transfer*, 81, 13-18.